Journal of Hazardous Materials 194 (2011) 100–108

Contents lists available at ScienceDirect

Journal of Hazardous Materials

journal homepage: www.elsevier.com/locate/jhazmat

Feasibility study of a photocatalytic reactor for in situ groundwater remediation of organic compounds

L.L.P. Lim*, R.J. Lynch**

Department of Engineering, University of Cambridge, Trumpington Street, Cambridge CB2 1PZ, United Kingdom

ARTICLE INFO

Article history:
Received 18 April 2011
Received in revised form 24 June 2011
Accepted 21 July 2011
Available online 5 August 2011

Keywords:
Cumulative performance
Ethylbenzene
MTBE
o-Xylene
Sand tank experiment
Toluene

ABSTRACT

Remediation of groundwater contaminated by gasoline leakage from underground structures is usually complicated and costly. This work describes the use of an underground reactor, in a sand tank, placed downgradient from a simulated leakage of MTBE and other gasoline components. The reactor, Honeycomb I, is full scale in the horizontal plane. It tested the remediation of MTBE plumes at various velocities and in the presence of other gasoline compounds (toluene, ethylbenzene and o-xylene – TEo-X). The overall performance of Honeycomb I was evaluated and the efficiencies of two different experimental scales were compared. The MTBE plume was longer but narrower with increasing groundwater to MTBE velocity ratio. MTBE appeared to have a minor co-solvent effect on the TEo-X migration as TEo-X migrated at the MTBE migration rate but at significantly low concentrations. The MTBE removal efficiency decreased by about 8% in the presence of TEo-X. The scaled up Honeycomb I successfully treated 212 L of groundwater in 24 days and demonstrated its reliability over a 10-month period, achieving an overall 76% MTBE removal. In essence, this study demonstrated the potential of the immobilised photocatalytic reactor for in situ groundwater remediation, at the velocities tested in this study.

1. Introduction

Remediation of contaminated groundwater is a complicated engineering problem, particularly for contaminants which are mobile and persistent in the environment such as methyl tert butyl ether (MTBE). MTBE, the target contaminant in this study, is a contaminant of concern as it causes unpleasant taste and odour at concentration as low as 20 $\mu g\,L^{-1}$ [1,2], making water undrinkable. Most existing clean-up technologies are affected by soil heterogeneity, especially those involving water withdrawal (pump-and-treat), vapour withdrawal (soil vapour extraction) or air/vapour injection (air sparging and thermal treatment). In addition to soil heterogeneity problems, in situ bioremediation including natural attenuation is often too slow for cases when urgent remediation is required such as clean-up near to drinking water sources. On the other hand, in situ chemical oxidation (ISCO), such as hydrogen peroxide and ozone oxidation with UV [3], can rapidly oxidise contaminants and is thus suitable for emergency clean-up of accidental spills. However, the reaction may be too rapid for clean-up of gradual and continuous leakages of contaminants from underground storage tanks and pipelines.

Groundwater remediation technologies including advanced oxidation processes are also affected by the presence of other groundwater constituents. While the presence of some constituents can inhibit bioremediation [4], ISCO can become costly for sites with high oxidisable (organic and inorganic) content as more chemicals need to be injected and excessive chemical injection may lead to violent reaction in the subsurface [5]. Both in situ bioremediation and ISCO may produce more hazardous by-products. A common reason for the inhibition of efficiency is associated with the extra competition for oxidising or reducing agents by other compounds.

Photocatalysis is an advanced oxidation process in which UVA light stimulates the formation of hydroxyl radicals on the photocatalyst surface in the presence of oxygen. It has been proven effective in degrading a plethora of organic compounds over the past decades [6–9], including MTBE [10,11] and toluene, ethylbenzene and o-xylene (TEo-X) [12]. Although photocatalysis is less rapid than ISCO, its reaction rate matches well with groundwater velocities of a few $cm\,d^{-1}$. Its advantages over other technologies include (i) environmentally friendly: a complete photocatalytic degradation of organic compound produces carbon dioxide, water and simple mineral acid for ecological uptake, (ii) a controllable process: a photocatalytic reaction only occurs in the presence of UVA light, air and photocatalyst, (iii) reaction rate: the photocatalytic degradation rate of organic compound is significantly faster

* Corresponding author. Department of Civil Engineering, Faculty of Engineering, Universiti Malaysia Sarawak (UNIMAS), 94300 Kota Samarahan, Sarawak, Malaysia.
** Corresponding author. Tel.: +44 0 1223 332714; fax: +44 0 1223 339713.
E-mail addresses: llpl2cam@gmail.com, llpl2@cam.ac.uk (L.L.P. Lim), rjl1@eng.cam.ac.uk (R.J. Lynch).

0304-3894/$ – see front matter © 2011 Elsevier B.V. All rights reserved.
doi:10.1016/j.jhazmat.2011.07.087

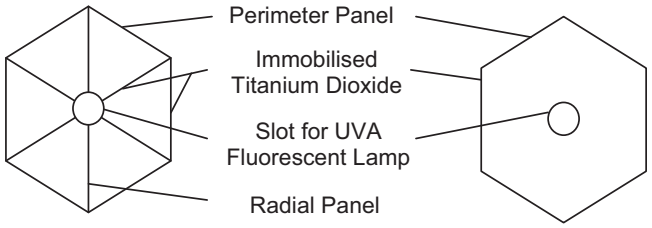

Fig. 1. Plan view of the reactor used in the sand tank experiment, Honeycomb I (left) and in the column reactor, Honeycomb II (right) [18].

than that of biodegradation [13,14], (iv) material: the photocatalyst, titanium dioxide (TiO_2), is non-toxic and can be regenerated via UVA light illumination in clean water in the presence of oxygen or calcination at 500 °C [8], and (v) availability: TiO_2 is commercially produced, thus, the cost is affordable. Therefore, the application of photocatalysis in a trench is proposed to overcome the limitation of contaminant removal efficiency due to soil heterogeneity.

To the authors' knowledge, in situ groundwater clean-up using photocatalysis is a novel approach. Some studies incorporated photocatalytic attenuation of MTBE into a pump-and-treat system, i.e. slurry falling film reactor [15]. Mehos and Turchi [16] used a field scale concentrating solar photocatalytic reactor (slurry) to treat the extracted TCE-contaminated groundwater. Sahle-Demessie et al. [17] suggested an immobilised photocatalytic reactor to be used for groundwater remediation. Previously, a model of the proposed immobilised photocatalytic reactor design in this research, Honeycomb II, has demonstrated its potential for in situ MTBE attenuation in a 4 L column reactor [11,12]. Therefore, Honeycomb I was scaled up from 100 mm i.d. Honeycomb II [11,12,18] to 200 mm i.d. (field scale dimension) and incorporated into a sand tank to simulate the in situ clean-up of MTBE plume near a gasoline spillage. Honeycomb II has catalyst sheets lined internally on the hexagonal structure only, while Honeycomb I has additional catalyst sheets arranged perpendicularly around the UVA lamp as radial panels which increases the surface area to volume ratio (Fig. 1), in order to ensure a good clean-up. Although the tank correctly models the field scale in the horizontal plane, the depth of the tank, 0.3 m, is much less than the expected field scale depth (2 m). This modular scale up study is intended to validate the efficiency of an actual field scale photocatalytic reactor design in an emulated field condition by testing an individual (horizontal) segment of a photocatalytic reactor system in a sand tank. Therefore, the results of the smaller model, Honeycomb II from previous studies [11,12,18] are used as reference.

In a laboratory scale sand tank, it is possible to investigate the parameters which influence the performance of the clean-up. In addition to providing more relevant information, a simple and systematic laboratory scale study is less risky than a field test as it is (i) more economical to evaluate in smaller experimental dimension (a horizontal segment of the full scale module), (ii) difficult to obtain a well characterised site in terms of hydrogeology, and (iii) manageable experimental parameters and shorter experimental duration allows variation of experiments. The sand tank represents a horizontal (22 cm) slice of the full scale reactor, which can be as deep as 2 m. The MTBE plume is simulated by injecting MTBE into the tank to emulate a leakage from underground storage tank. The objective of generating an MTBE plume is to test the clean-up process at various flows, rather than to examine the plume itself in detail. The groundwater velocities applied in this study are based around the 9 cm d^{-1} obtained in the Borden aquifer [19]. The plume behaviour in the sand tank is constricted by the tank, but it still provides a reasonably realistic clean-up test.

The second part of this study evaluated the effect of other gasoline type organic compounds (15.6TEo-X experiment) on the migration and removal of MTBE. Generally, the photocatalytic efficiency is not only inhibited by the competition for oxidising or reducing agents but also the competition for adsorption by the more strongly adsorbed molecules and scavenging of radicals or holes on the catalyst surface. Both will reduce the number of oxidising agents on the catalyst surface. Lim and Lynch [11] found that the presence of other organic or inorganic constituents inhibited the photocatalytic degradation rate of MTBE, which was in agreement with Butler and Davis [20], Liao et al. [21], Sahle-Demessie et al. [15] and Klauson et al. [22]. The inhibition of the photocatalytic degradation of MTBE by organic constituents is mainly associated with the competition for adsorption on the catalyst surface, thus the more strongly adsorbed compounds are degraded first, suppressing the adsorption and subsequent degradation of MTBE.

2. Material and methods

2.1. Sand tank experiment

The laboratory scale sand tank (Fig. 2b–d) consists of an inlet chamber, sand chamber, reactor chamber and outlet chamber. It has a dimension of 980 mm (L) × 200 mm (W) × 305 mm (H), where the effective lengths are 500 mm and 330 mm for sand and reactor chambers, respectively. The tank width of 200 mm is the same as the photocatalytic reactor width. The groundwater depth is about 220 mm. The chambers are partitioned by 10 mm thick perforated Perspex lined with 60 μm stainless steel mesh on the side facing the sand. The inflow chamber was filled with only deaired deionised water to: (i) provide uniform flow across the section area of the tank, (ii) prevent possible air trapped in the inlet tube from entering and becoming trapped in the sand chamber and (iii) allow settlement of any particles which might clog the screen or mesh partition. The sand chamber allows the plume to develop in a leaking tank simulation. The reactor chamber, with partitions acting as the walls of a trench, contains catalyst sheets illuminated by a 15 W Philips Cleo UVA fluorescent lamp (Honeycomb I). The space around Honeycomb I was filled with sand (Section 2.3), which functions as a sand filter to minimise turbidity in the reactor by preventing fine particles from entering the reactor. The flow through the tank is controlled by the difference in hydraulic head between inlet and outlet chambers. When used for MTBE removal, the tank was covered by a 10 mm thick Perspex lid and the sampling points were sealed using PTFE sheets to prevent emission of vapour from the sand tank.

The tank has a total of 32 sampling points spaced out at 16 locations (Fig. 2b, Table 1) at two depths of 60 and 120 mm (below water level) for each location (Fig. 2c), with two sampling points are located in the photocatalytic reactor (Fig. 2b). The sampling ports consist of stainless steel tubes; the withdrawal point of sample in the sand was covered with 60 μm stainless steel mesh to minimise intrusion of sand particles, which can affect the sampling. The samples were withdrawn from the sampling ports using a modified 10 mL glass syringe, with a 220 mm long 0.8 mm i.d. stainless steel tube. Stainless steel and a glass syringe were used to minimise corrosion and prevent adsorption of MTBE and TEo-X during sampling, respectively.

2.2. Photocatalytic reactor

The Honeycomb I reactor has an internal hexagonal cross section of 200 mm, which is the proposed full scale in plan view (horizontal slice) but not in the vertical section. Its hexagonal cross section enables the merging of reactors for serial clean-up in the field to achieve the desired level. The reactor concept has been detailed in a previous paper [18]. The UVA light intensity at 100 mm away

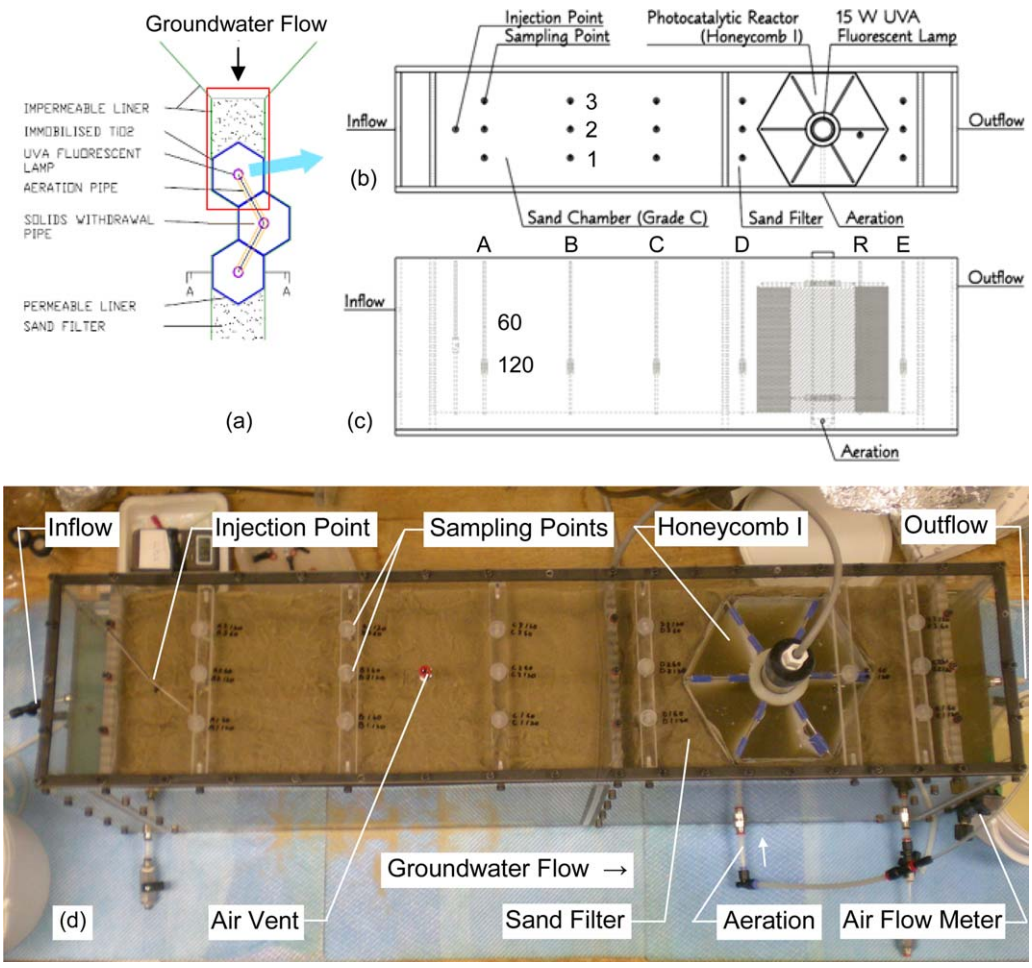

Fig. 2. (a) Plan view of intended application on site showing how hexagonal units can be linked together in series to achieve the required clean-up level, (b) plan view of the sand tank, which examines the clean-up using a single hexagonal unit (Honeycomb I), (c) side view of the sand tank showing the inflow and outflow chambers, sampling points and reactor, and (d) photo showing the plan view of the sand tank after installation and the location of sampling points.

from a 15 W Philips Cleo UVA fluorescent lamp is approximately 0.3 mW cm^{-2}, measured at a peak wavelength of 365 nm using a UVItec RX-003 radiometer. The catalyst sheets were arranged both around the perimeter of the hexagon and radially around a 50 mm i.d. borosilicate glass sleeve, which encloses the UVA lamp (Fig. 2d). The catalyst sheets consist of woven fibreglass which were dip-coated in a mixture of TiO_2 (Aeroxide TiO_2 P25 and sol–gel) [18,23]. The 100 g m^{-2} woven fibreglass was initially heat treated at 500 °C for 1 h to remove possible organic impurities on its surface and making it slightly stiffer and more manageable. Then, it was dip-coated 5 times prior to drying at 100 °C for 1 h to remove moisture content, followed by ramping at 5 °C min^{-1} and held at 500 °C for 1 h to transform the sol–gel crystal structure from amorphous to anatase, and to remove organic components. It should be noted that only a single set of catalyst sheets, coated 14 months previously, was used throughout this study. The total catalyst surface area is about 0.25 m^2, yielding a surface area to volume ratio of approximately 33.1 m^2 m^{-3}. The perforated hexagonal stainless steel structure was wrapped with a layer of 60 μm stainless steel mesh to prevent intrusion of sand particles into the photocatalytic reactor. Honeycomb I was submerged in the reactor chamber for approximately 10 months throughout this study.

The air flow was maintained at 0.2 L_a min^{-1} (L_a for litres of air), similar to that used in 100 mm i.d. reactor [12]. Consequently, the air flow to volume ratio was halved to 0.025 L_a min^{-1} L^{-1}, also to compensate for the larger width (cell diameter) to height (D/H) ratio in the larger scale reactor. Sufficient air is provided at this ratio as the complete photocatalytic degradation of 1 mg L^{-1} MTBE

Table 1
The coordinates and nomenclatures of sampling points.

Width, *y* (mm)	Depth, *z* (mm)	Distance from injection point, *x* (mm)					
		50	200	350	500	715	780
50	60	A160	B160	C160	D160		E160
	120	A1120	B1120	C1120	D1120		E1120
100	60	A260	B260	C260	D260	R60	E260
	120	A2120	B2120	C2120	D2120	R120	E2120
150	60	A360	B360	C360	D360		E360
	120	A3120	B3120	C3120	D3120		E3120

Note: Injection point coordinate: *x*, *y*, *z* = 35, 100, 90 mm.

Table 2
Flow profile applied in the sand tank experiments. Velocity refers to Darcy's velocity except for average linear velocity and porosity is 0.42.

Exp.	Groundwater Flow		MTBE injection		Total		Average linear velocity ($cm\,d^{-1}$)
	Flow ($mL\,min^{-1}$)	Velocity ($cm\,d^{-1}$)	Flow ($mL\,min^{-1}$)	Velocity ($cm\,d^{-1}$)	Flow ($mL\,min^{-1}$)	Velocity ($cm\,d^{-1}$)	
14.6	2.23	7.3	2.23	7.3	4.46	14.6	34.8
15.6	2.38	7.8	2.38	7.8	4.76	15.6	37.1
29.0	6.11	20.0	2.75	9.0	8.86	29.0	69.0
37.3	9.17	30.0	2.23	7.3	11.40	37.3	88.8

requires approximately 2.7 $mg\,L^{-1}$ dissolved oxygen. The agitation in the reactor by aeration was assumed to be similar for both scales, achieving complete mixing of solution. The flow into the tank is not a parameter of concern as it is typically laminar in both scales (without aeration) due to the slow groundwater flow. The scaled up reactor (cell diameter doubled; reactor volume approximately 7.6 L) has a larger surface area to volume ratio, which affects the mass transfer of contaminants, due to the relatively wider radial panels than that of its model (21.5 $m^2\,m^{-3}$ – Honeycomb I [18]).

2.3. Preparation of homogeneous aquifer

The deionised water was deaired (synthetic groundwater) as the ambient dissolved oxygen concentration in groundwater is typically below 2 $mg\,L^{-1}$ [24] and to minimise air trapped among the sand grains, which can hinder the passage of groundwater. Deaired deionised water was used as groundwater and to make the MTBE solution.

Graded sand of 125–500 μm dia. was used due to its (i) grain size within the range between 70 and 690 mm at Borden aquifer [19], (ii) permeability closer to that of Borden aquifer [19], and (iii) lower transverse dispersion to the sides of the tank to avoid the contaminant to flow from the sides of the tank. The sand was filled using the wet method, whereby the deaired deionised water was filled up to the outflow level prior to filling with sand, in order to (i) ensure no air bubbles trapped among sand grains, which would affect permeability, and (ii) enable water displacement test to obtain the sand volume. The permeability of the aquifer in the sand tank, evaluated using a constant head control device and measuring the flow, was approximately $5 \times 10^{-5}\,m\,s^{-1}$ (data not shown), which is similar to the mean permeability of $7 \times 10^{-5}\,m\,s^{-1}$ obtained at Borden aquifer [19] and within the range for medium to coarse sand, i.e. from 9×10^{-7} to $5 \times 10^{-3}\,m\,s^{-1}$ [25].

The flows for the experiments were selected based on the average linear velocity of approximately 9 $cm\,d^{-1}$ at Borden aquifer [19]. The groundwater flow and MTBE injection were controlled using Watson Marlow 323S/D peristaltic pumps because the simulated flow were too slow to be controlled using a head control device. The velocity of MTBE injection, v_{MTBE}, was calculated (similar to groundwater velocity, v_{gw}) by assuming the plume conveyed through the whole cross section area of the saturated sand, A (0.044 m^2), for simple estimation of plume migration and velocity ratio to simulate leakage from underground storage tank ($v_{MTBE} = Q/A$). The velocities used are summarised in Table 2 and of the order in Table 4. 15.6 V refers to the experiment to validate the clean-up efficiency of the reactor for 14.6, prior to 15.6TEo-X. Groundwater flow was continued at a water velocity of 2.2 $cm\,d^{-1}$ in between experiments.

2.4. Preparation and analysis of contaminants

MTBE is often found in groundwater together with gasoline. Therefore, toluene, ethylbenzene and o-xylene (TEo-X) were used to represent gasoline type organic compounds, as most studies on co-occurrence of MTBE with organic compounds were focused on BTEX [26,27]. The TEo-X concentrations were determined from the highest concentrations (toluene: 30, ethylbenzene: 10 and o-xylene: 20 $mg\,L^{-1}$) used in a previous study [12]. MTBE

Table 3
Experimental phases for the sand tank experiment.

Experimental phase	Configuration			Monitoring of contaminant concentration		Remarks
	Injection of contaminant solution	Air supply on	UVA light on	Sand aquifer[a]	In the reactor	
Migration	Yes	No	No	Yes	No	• To observe the contaminant migration in homogeneous sand • Reactor assumed as a "well" when no treatment was applied
Aeration	Yes	Yes	No	No	Yes	• To completely mix the plume to obtain uniform concentration in the reactor and to observe reduction of contaminant concentration due to aeration only • Begin after concentration in row E has stabilised
Photocatalytic reaction	Yes	Yes	Yes	No	Yes	• To observe reduction of contaminant concentration due to photocatalytic reactor • Begin after 6–7 h of aeration
Flushing	No	Yes	Yes	Yes	No	• To observe the clearing of the contaminant plume • Begin when the contaminant concentration in the reactor and row E has stabilised

Note: Batch sampling of the whole sand tank is conducted once daily, except thrice daily in the migration and flushing phases.
[a] Sand aquifer refers to the component outside the reactor (row A, B, C, D and E in Fig. 1b).

Table 4
Sand tank experimental details and performance of Honeycomb I.

Total Velocity ($cm\,d^{-1}$)	HRT (d)	Total duration (h)	Reaction duration[a] (h)	Volume treated (L)	$C_{0\,MTBE}$ [b] ($mg\,L^{-1}$)	MTBE removal (%)	MTBE removed (mg)	k_{MTBE} (h^{-1})	R^2
14.2[c]	1.00	8	8	8	~80	84.0	538	0.253	0.95
29.0[d]	0.60	69	45	23.9	–	–	–	–	–
14.6	1.18	216	120	32.1	~41	88.1	1160	0.106	0.98
29.0	0.60	194	74	39.3	~30	72.3	853	0.073	0.98
37.3	0.46	120	48	32.8	~20	61.9	406	0.091	0.98
15.6 V	1.11	220	148	42.3	~32	79.2	1072	0.045	0.99
15.6 TEo-X	1.11	240	147	42.0	~30	71.3	898	0.040	0.95
Total		1039	582	212.4		76.2	4389[e]		

[a] Reaction duration include aeration phase as aeration is an essential component of photocatalysis.
[b] The initial MTBE concentration in Honeycomb I reactor after aeration phase was initiated (assumed completely mixed).
[c] Data from batch experiment using 100 mm (i.d.) Honeycomb II in a 4 L column reactor [11] for comparison with sand tank experiment at total velocity of 14.6 $cm\,d^{-1}$; not included in the total for sand tank experiments.
[d] Trial experiment, the MTBE removal efficiency was not known as the reactor was switched on when the MTBE plume just reached the reactor. The final concentration stabilised at about 6 $mg\,L^{-1}$.
[e] The total amount of MTBE removed did not include the amount removed in the trial experiment as it was unknown.

concentration was 100 $mg\,L^{-1}$. In the 15.6TEo-X experiment, the contaminant solution was prepared by spiking MTBE and TEo-X into deaired deionised water. The contaminant solution was injected into the sand tank prior to the flushing phase. MTBE and TEo-X concentrations were measured using an Agilent 6850 series gas chromatograph with flame ionisation detector.

2.5. Experimental phases

The sand tank experiment consists of four phases, i.e. migration, aeration, photocatalytic reaction and flushing (Table 3). The groundwater is pumped into the tank via the inflow (Fig. 2b) throughout the experiment. The contaminant is injected continuously until the flushing phase. The sampling during the migration and flushing phases is focused in the sand chamber to obtain the breakthrough curve of contaminants at various sampling points for characterisation of contaminant migration. The sampling during the aeration and photocatalytic reaction phases is focused in the photocatalytic reactor to obtain the reduction of contaminant concentration.

3. Results and discussion

The results from the sand tank experiments are presented in the order of the respective experimental phases (Table 3) from Sections 3.1 to 3.4. The cumulative performance evaluation and observation of Honeycomb I over the 10-month study is discussed in Sections 3.5 and 3.6. The scale up of the photocatalytic reactor is evaluated in Section 3.7 by comparing the performance of Honeycomb I with its model, Honeycomb II from previous studies [11,12].

3.1. Migration of contaminants

In order to observe how the contaminant plume spreads in the sand tank, concentrations of the respective contaminants were plotted against the coordinate of the sampling points at sampling depths of 60 and 120 mm at various times. The concentration distribution was plotted via interpolation of concentrations recorded at two points using Matlab. Fig. 3 shows a typical concentration plot of MTBE and TEo-X plumes at a total velocity of 15.6 $cm\,d^{-1}$.

Concentration plots of the MTBE plume in sand tank experiments at various velocities showed that MTBE migrated faster with increasing v_{gw}:v_{MTBE} ratio. At velocities of 14.6, 29.0 and 37.3 $cm\,d^{-1}$, MTBE was detected after 24 h of MTBE injection in rows C, D and R, respectively. The MTBE plume was longer but narrower with increasing v_{gw}:v_{MTBE} ratio, indicating more longitudinal and less transverse dispersion, as expected [28]. The MTBE plume width was broader at lower v_{gw}:v_{MTBE} ratio because the injected MTBE would disperse "radially", prior to being transported by the regional groundwater. The MTBE concentration especially along the midline (y = 100 mm) stabilised at circa 90 $mg\,L^{-1}$ (90% C/C_0), in all the sand tank experiments. MTBE migration at the velocity of groundwater indicated that the migration was advection dominated.

In the 15.6TEo-X sand tank experiment, the migration of TEo-X was similar to that of MTBE but at significantly lower concentration. The maximum toluene, ethylbenzene and o-xylene concentrations detected in the tank were about 4, 1.5 and 3 $mg\,L^{-1}$, i.e. about 15% of their respective initial concentrations (Fig. 3). The migration of the more retarded hydrocarbons in water, TEo-X, could have been assisted by MTBE via a co-solvent effect, which agrees with Chen et al. [29] who showed that MTBE mobilised polynuclear aromatic hydrocarbon from contaminated soil. The co-solvent effect is the increase of hydrocarbon solubility by a highly soluble organic solvent in water, resulting in the increase of concentration and migration of the more retarded hydrocarbons in water.

3.2. Effect of aeration on the vaporisation of contaminants

The aeration phase was conducted to observe and distinguish between the vaporisation and the degradation of MTBE. When the reactor was aerated, MTBE concentrations at both depths were similar, indicating complete mixing by aeration. Fig. 4 shows the reductions of MTBE concentration (normalised by the initial concentration) in the aeration and reaction phase in Honeycomb I at four velocities. Immediately after the aeration phase started, the initial MTBE concentration in the reactor ($C_{0\,MTBE}$) in the 14.6, 15.6 V, 15.6TEo-X, 29.0 and 37.3 experiments was approximately 41, 32, 30, 30 and 20 $mg\,L^{-1}$, respectively. The initial MTBE concentration in the reactor reduces with the increasing v_{gw}:v_{MTBE} ratios (Table 2) of approximately 1:1, 2:1 and 4:1. A higher v_{gw}:v_{MTBE} ratio resulted in more dilution in the reactor as a greater fraction of water flows through the reactor, which concurred with the narrower MTBE plume at the higher v_{gw}:v_{MTBE} ratio.

During the aeration phase, the reduction of MTBE concentration fluctuated, which differed from the steady exponential reduction observed when the UVA lamp was switched on. Vaporisation by aeration appeared to be independent of the total velocity. The percentages of MTBE removed by 0.2 $L_a\,min^{-1}$ air flow at velocities of 14.6, 29.0 and 37.3 $cm\,d^{-1}$ were approximately 30 (6 h), 25 (7 h) and 33 (7 h) %, respectively (Fig. 4). These are slightly higher than the 20% MTBE removal observed at 0.2 $L_a\,min^{-1}$ (0.05 $L_a\,min^{-1}\,L^{-1}$)

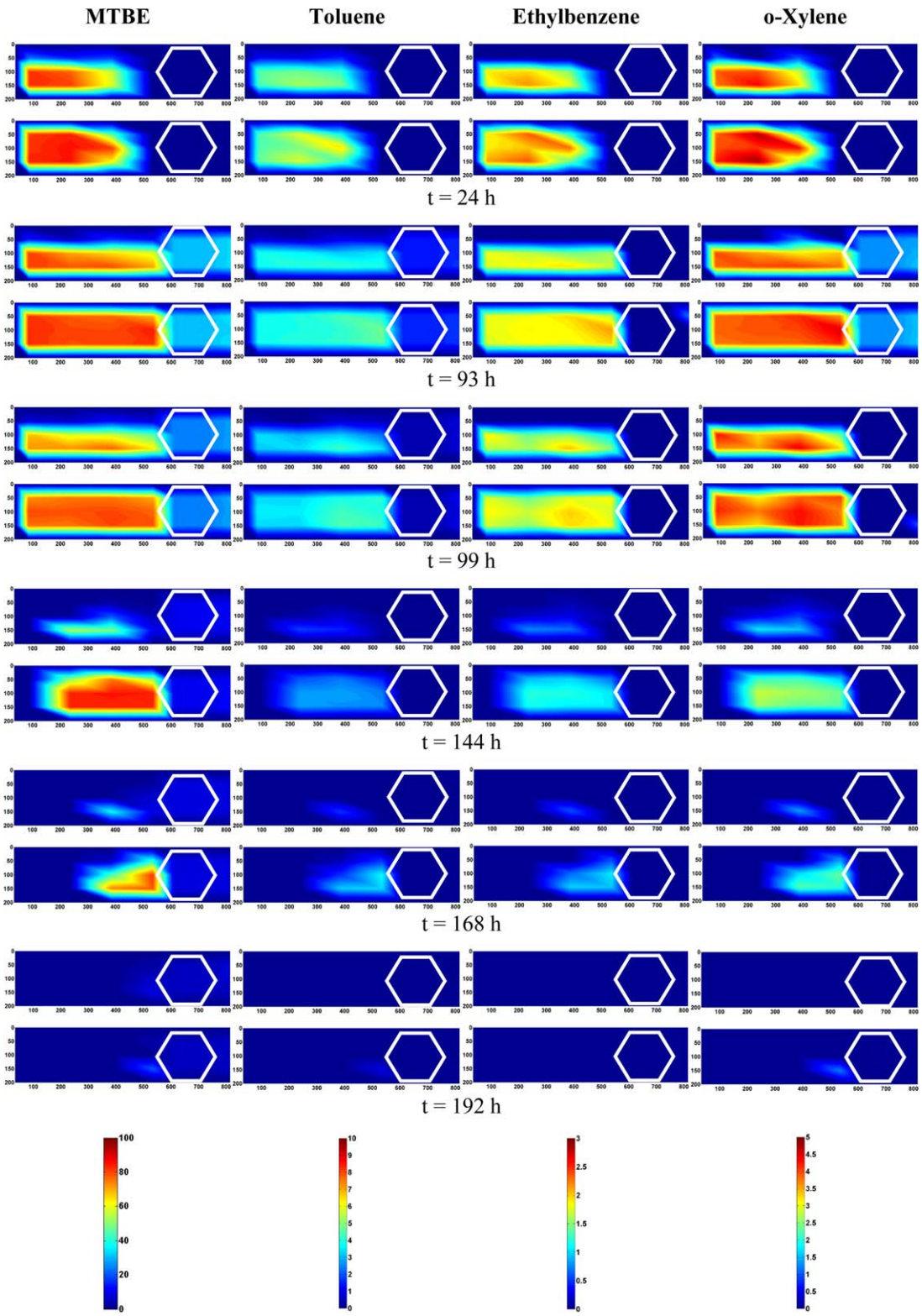

Fig. 3. Surface plot of concentration showing the migration of the organic compounds in the sand tank at a velocity of 15.6 cm d^{-1}. The migration of toluene, ethylbenzene and o-xylene is similar to that of MTBE, implying that the migration of toluene, ethylbenzene and o-xylene in the tank is assisted by MTBE via the co-solvent effect. TEo-X concentrations obtained at the sampling points were about 10–15% of the initial concentration injected into the sand tank.

in the 4 L column reactor [12] (Please refer to Appendix A for the results of the control batch experiment for aeration), in which the D/H ratio is half that of the present one. The effect of aeration on the MTBE vaporisation in the reactor increases with increasing air flow to volume ratio and D/H ratio [11]. Vaporisation via aeration should be considered as part of the overall photocatalytic reactor efficiency, as aeration is an essential component of a photocatalytic reactor system.

In the 15.6TEo-X experiment, the initial TEo-X concentration in the reactor totalled to 3.2 mg L^{-1}, mainly consisting of toluene and

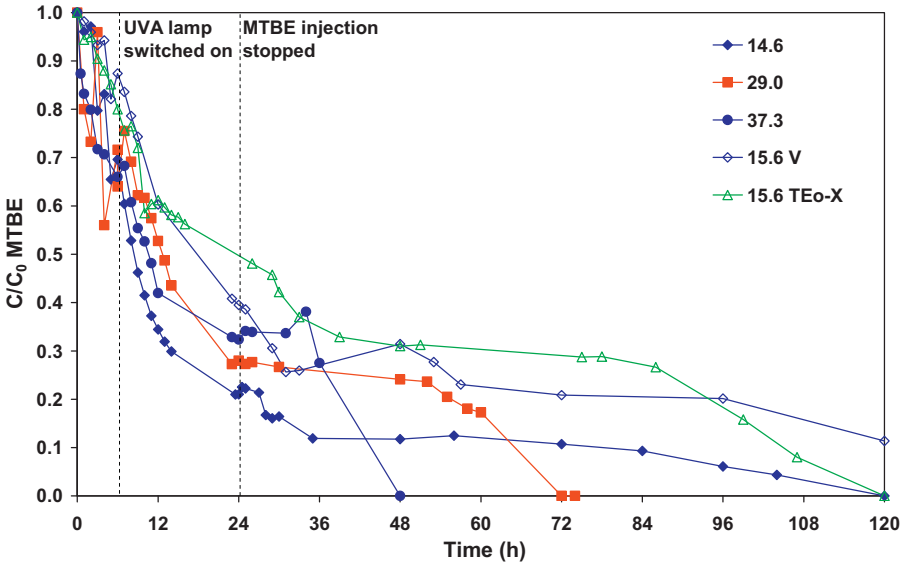

Fig. 4. Reduction of MTBE concentration in the reactor (average of R60 and R120) from the initiation of the aeration phase. The aeration and UVA lamp was switched on at 96 h, 102 h (14.6); 120 h, 127 h (29.0); 72 h, 79 h (37.3); 72 h, 78 h (15.6 V); 93 h, 99 h (15.6 TEo-X), respectively, after MTBE injection started (refer to Table 2 for flow details). Experimental conditions: continuous air flow: 0.2 L_a min^{-1}; UVA lamp on; room temperature: 20 °C; C_0: please refer to $C_{0\,MTBE}$ in Table 4.

o-xylene. Ethylbenzene concentration was below detectable limit within the first hour of aeration possibly due to its low initial concentration, followed by o-xylene after 4 h. About 0.4 mg L^{-1} toluene remained after 6 h of aeration.

3.3. Photocatalytic degradation of contaminants

The third phase of the sand tank experiment, i.e. the reaction phase, was initiated when the UVA lamp was switched on. The clean-up appeared to be localised within the reactor and did not affect the MTBE or TEo-X concentration prior to the reactor (t = 99 h in Fig. 3 – MTBE/TEo-X). This indicated that the photocatalytic reaction is contained within the reactor in the presence of UVA light, air and TiO_2. This can be an advantage particularly when groundwater remediation is required in environmentally sensitive areas, for instance aquifer preservation and agricultural lands.

Fig. 4 shows the reduction of MTBE concentration in Honeycomb I from the initiation of the aeration phase. It should be noted that the time of reactor operation in Fig. 4 was reset to the time when aeration was initiated in the reactor, for comparison purposes. The UVA lamp was switched on after 6, 6, 6, 7 and 7 h of aeration during the 14.6, 15.6 V, 15.6TEo-X, 29.0 and 37.3 experiments, respectively. It shows that the MTBE removal efficiency reduces with increasing water velocity. Table 4 summarises the experimental details and performance of Honeycomb I in all the sand tank experiments for comparison purposes, as well as providing the cumulative performance of the reactor. The MTBE removal efficiency was 88.1, 79.2, 71.3, 72.3 and 61.9% at total velocities of 14.6, 15.6 V, 15.6TEo-X, 29.0 and 37.3 cm d^{-1}, respectively. Higher MTBE removal was achieved at lower velocities due to the longer hydraulic residence time (HRT) for the photocatalytic degradation of MTBE molecules in the reactor [11]. Despite the lower initial MTBE concentration in the reactor at higher v_{gw}:v_{MTBE} ratios, the MTBE removal efficiency can be compared directly because the photocatalytic degradation of MTBE is a pseudo first order reaction.

The lower MTBE removal efficiency in the 15.6 V experiment compared to that of 14.6 was possibly due to the gradual wearing of the catalyst performance, which could be due to gradual deactivation of active sites on the catalyst surface by adsorbed compound molecules and some detachment of catalyst; considering that Honeycomb I was submerged in the tank for 10 months. There was some adsorption on the catalyst surface as the catalyst surface was slightly brownish like the sand colour when Honeycomb I was not operated for approximately 4 months after the second sand tank experiment, which was similar to the catalyst in Honeycomb I after completing all the sand tank experiments (Fig. 5a). The slightly higher velocity in the 15.6 V experiment was unlikely to have significant impact on the MTBE removal efficiency of Honeycomb I as the HRT was 1.1 day, which was more than the critical HRT of 1 day. The catalyst performance can be recovered via UVA light irradiation in clean water in the presence of oxygen or baking the catalyst at 500 °C [8].

In the presence of TEo-X, the MTBE removal efficiency decreased about 7.9% to 71.3%, which was consistent with the decrease of about 9.1% in the presence of 20 mg L^{-1} TEo-X found previously using Honeycomb II [12]. Honeycomb II does not have radial panels of catalyst (Fig. 1). The MTBE removal efficiency of Honeycomb I was not affected as significantly as Honeycomb II due to the significantly lower TEo-X concentrations, mainly toluene and o-xylene, and the absence of dissolved ions. It is likely that the presence of TEo-X affected the MTBE removal efficiency due to the competition for adsorption by the more strongly adsorbed TEo-X molecules on the catalyst surface, leading to its degradation prior to MTBE molecules and inhibiting the degradation of MTBE [12,15].

3.4. Flushing of contaminants

When the contaminant concentration in the reactor and row E became constant, the flushing phase was initiated by stopping the injection of contaminant. All the contaminants cleared out at the end of the sand tank experiments (last row in Fig. 3). The second last row in Fig. 3 (t = 168 h) shows that MTBE and TEo-X migrated at similar rates, which is in agreement with the earlier mentioned co-solvent effect.

3.5. Cumulative performance of Honeycomb I

Table 4 shows the details of the sand tank experiments and performance of Honeycomb I throughout this study over 10 months [30]. The total effective experimental duration was 1039 h. Honeycomb I was operated up to 582 h, removing about 4389 mg MTBE

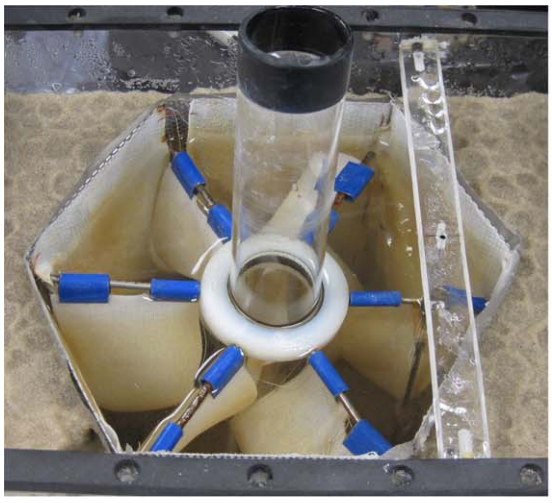

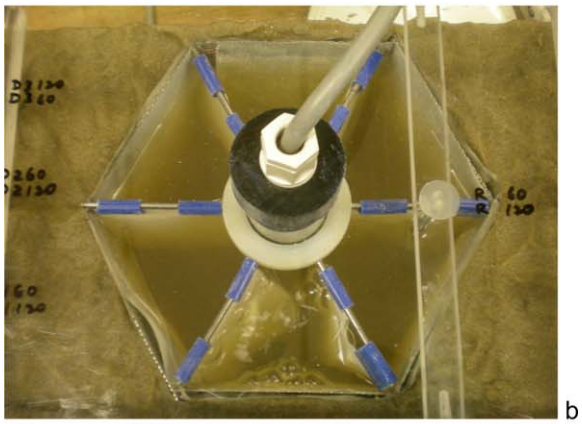

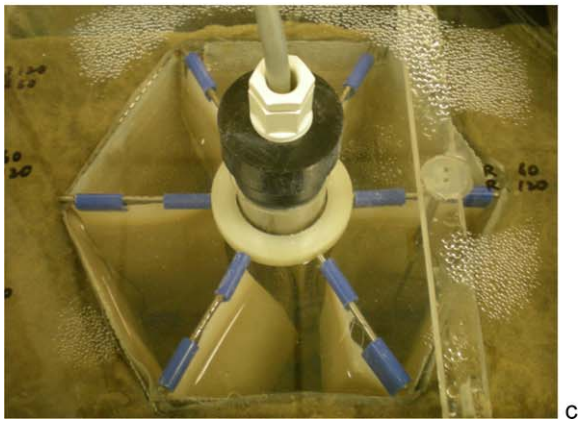

Fig. 5. (a) The catalyst surface was slightly brown like the sand colour 10 months after the reactor was installed and including six sand tank experiments, (b) Honeycomb I after installation and (c) Honeycomb I after two sand tank experiments.

(overall 76.2% MTBE removal) from the 212.4 L of contaminated groundwater treated.

The MTBE removal efficiencies in 15.6 V and 15.6TEo-X were less than 20% lower than that of 14.6, despite the fact that the MTBE photocatalytic degradation rate constant in both experiments was less than half that of 14.6. Despite the efficiency decrease after being submerged for 10 months, Honeycomb I still achieved 71.3% MTBE removal in the presence of TEo-X. This demonstrated that the immobilised catalyst is sufficiently durable at these velocities. Therefore, this scale up experiment can be considered successful in terms of performance and reliability.

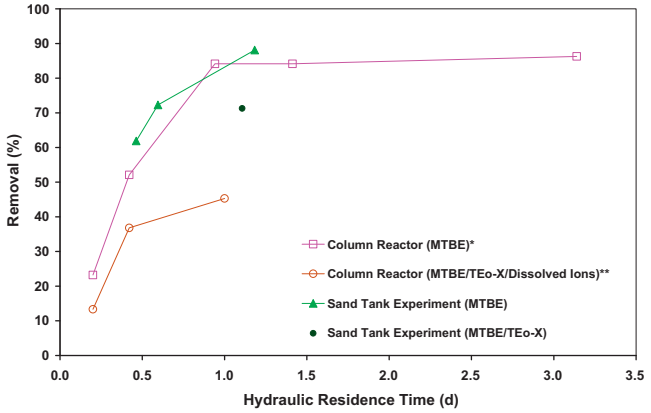

Fig. 6. MTBE removal efficiency of the column reactor (Honeycomb II) and sand tank reactor (Honeycomb I) at various HRTs, in both cases of MTBE only and MTBE with TEo-X. * Ref. [11], ** Ref. [12].

3.6. Honeycomb I observation

Fig. 5b shows the water in Honeycomb I was slightly turbid after its installation. However, the turbidity in Honeycomb I reduced (Fig. 5c) as more water flowed through the tank, indicating the sand filter and 60 μm stainless steel mesh are adequate in separating larger particles from entering Honeycomb I and minimising the turbidity, which can affect the efficiency by inhibiting UVA light from illuminating the catalyst surface. The turbidity and UVA light transmission in Honeycomb I after all the sand tank experiments (Fig. 5a) was below 10 NTU and more than 85%, respectively.

3.7. Comparison of reactor performance with its model reactor

Fig. 6 shows the MTBE removal efficiency of Honeycomb configurations at various HRTs tested in the flow study in a column reactor (100 mm i.d.) [11,12] and this sand tank (200 mm i.d.) [30]. HRT refers to the average duration for a contaminant molecule to remain in the reactor. Both reactors were operated at similar HRTs in order to validate the trend. The MTBE removal percentage increased with the HRT, which varies inversely with velocity. The critical HRT appears to be 1 day for both reactor scales. The scale up of Honeycomb I appears to be successful as it achieved a similar MTBE removal percentage to that of the column reactor when only MTBE was present [11]. Nevertheless, it should be noted that the MTBE removal efficiencies in the column reactor were achieved after 8 h, while the ones in the sand tank experiments were achieved after 24 h.

The generic trends obtained for both scales (Fig. 6) could provide a basis for the design of future systems, once the local groundwater flow and contaminant levels have been established. As the groundwater velocity in a trench is governed by the natural gradient, this plot is a useful reference in monitoring the performance of the reactor in the field. Since the area perpendicular to the groundwater flow and the photocatalytic reactor volume are known, the groundwater velocity can be converted to HRT (Eq. (1)).

$$\tau = \frac{V_R}{\nu \times A} \quad (1)$$

where τ is the HRT (d), V_R is the volume of a single photocatalytic reactor (m^3), ν is the groundwater (Darcy) velocity ($m\,d^{-1}$) and A is the cross-sectional area of a single photocatalytic reactor perpendicular to the groundwater flow (m^2).

Considering the presence of organic compounds and dissolved ions, a similar trend between the MTBE removal efficiency and HRT was obtained (Fig. 6), except with lower MTBE removal efficiencies [12]. Since the trend appeared consistent from three flow studies,

a sand tank experiment was conducted in the presence of TEo-X, only at the critical HRT of 1 day. A lower MTBE removal efficiency is expected because the presence of other oxidisable constituents is likely to compete with MTBE for adsorption sites on the catalyst surface. Nevertheless, the reduction of Honeycomb I efficiency in the sand tank (Fig. 6) was not as significant as that of Honeycomb II in the column reactor [12] due to the lower TEo-X concentration and also the absence of dissolved ions in Honeycomb I.

4. Conclusions

This study successfully simulated the clean-up of MTBE plumes using Honeycomb I in a sand tank and also demonstrated its efficiency in a relatively long term. TEo-X migrated through the sand chamber at similar rates to that of MTBE but at significantly lower concentrations, probably due to a co-solvent effect. Honeycomb I was operated in the sand tank for 10 months throughout this study, using one set of catalyst for 582 h (~24 days) and achieved an overall 76.2% MTBE removal, treating 212.4 L contaminated water. Some reduction in the efficiency of Honeycomb I was observed after being submerged in the sand tank for 10 months, possibly due to gradual deactivation of active sites on the catalyst surface by adsorbed compound molecules and some catalyst detachment. The photocatalytic degradation of MTBE was inhibited by the presence of TEo-X in the sand tank, which agreed with the observations in previous studies. The reliability of the scaled up reactor can be considered as a successful development for in situ groundwater remediation. The similar trend of reactor efficiency against HRT in both scales of reactor indicates that the reactor performance in the field can be simulated in a column reactor. Nevertheless, the efficiency of this novel reactor design can still be further improved, especially in terms of the quality of immobilised catalyst and the fine tuning of the UVA light irradiation and dimensions of Honeycomb I via pilot studies in the field.

Acknowledgements

We would like to thank Prof Malcolm Bolton for his kind advice in this study. We would also like to thank the Editor and reviewers for their constructive suggestions in improving the quality of this article. We are grateful to Cambridge Commonwealth Trust (CCT) and Tunku Abdul Rahman Sarawak Foundation Scholarship for the financial support and Evonik for their donation of the Aeroxide TiO_2 P25 photocatalyst.

Appendix A. Supplementary data

Supplementary data associated with this article can be found, in the online version, at doi:10.1016/j.jhazmat.2011.07.087.

References

[1] R. Johnson, J. Pankow, D. Bender, C. Price, J. Zogorski, MTBE to what extent will past releases contaminate community water supply wells? Environ. Sci. Technol. 34 (2000) 2A–9A.
[2] J. Jacobs, J. Guertin, C. Herron, MTBE Effects on Soil and Groundwater Resources, CRC Press Inc., Florida, 2001.
[3] T. Garoma, M.D. Gurol, O. Osibodu, L. Thotakura, Treatment of groundwater contaminated with gasoline components by an ozone/UV process, Chemosphere 73 (2008) 825–831.
[4] R.A. Deeb, K.M. Scow, L. Alvarez-Cohen, Aerobic MTBE biodegradation: an examination of past studies current challenges and future research directions, Biodegradation 11 (2000) 171–186.
[5] US EPA, Technologies for Treating MtBE and Other Fuel Oxygenates, US EPA/National Service Centre for Environmental Publications (NSCEP), Cincinnati, U.S.A., 2004.
[6] A. Mills, R.H. Davies, D. Worsley, Water purification by semiconductor photocatalysis, Chem. Soc. Rev. 22 (1993) 417–425.
[7] M.R. Hoffmann, S.T. Martin, W.Y. Choi, D.W. Bahnemann, Environmental applications of semiconductor photocatalysis, Chem. Rev. 95 (1995) 69–96.
[8] D.S. Bhatkhande, V.G. Pangarkar, A.A.C.M. Beenackers, Photocatalytic degradation for environmental applications – a review, J. Chem. Technol. Biotechnol. 77 (2001) 102–116.
[9] J.-M. Herrmann, Heterogeneous photocatalysis: state of the art and present applications, Top. Catal. 34 (2005) 49–65.
[10] R.D. Barreto, K.A. Gray, K. Anders, Photocatalytic degradation of methyl-tert-butyl ether in TiO_2 slurries: a proposed reaction scheme, Water Res. 29 (1995) 1243–1248.
[11] L.L.P. Lim, R.J. Lynch, Hydraulic performance of a proposed in-situ photocatalytic reactor for degradation of MTBE in water, Chemosphere 82 (2011) 613–620.
[12] L.L.P. Lim, R.J. Lynch, In-situ photocatalytic remediation of MTBE-contaminated water: effect of organics and inorganics, Appl. Catal. A: Gen. 394 (2011) 52–61.
[13] S.R. Kane, H.R. Beller, T.C. Legler, C.J. Koester, H.C. Pinkart, R.U. Halden, A.M. Happel, Aerobic biodegradation of methyl tert-butyl ether by aquifer bacteria from leaking underground storage tank sites, Appl. Environ. Microbiol. 67 (2001) 5824–5829.
[14] B.N. Chisala, N.G. Tait, D.N. Lerner, Evaluating risks of methyl tertiary butyl ether (MTBE) pollution of urban groundwater, J. Contam. Hydrol. 91 (2007) 128–145.
[15] E. Sahle-Demessie, T. Richardson, C.B. Almquist, U.R. Pillai, Comparison of liquid and gas-phase photooxidation of MTBE: synthetic and field samples, J. Environ. Eng. 128 (2002) 782–790.
[16] M.S. Mehos, C.S. Turchi, Field testing solar photocatalytic detoxification on TCE-contaminated groundwater, Environ. Prog. 12 (1993) 194–199.
[17] E. Sahle-Demessie, J. Enriquez, G. Gupta, Attenuation of methyl tert-butyl ether in water using sunlight and a photocatalyst, Water Environ. Resour. 74 (2002) 122–130.
[18] L.L.P. Lim, R.J. Lynch, A proposed photocatalytic reactor design for in-situ groundwater applications, Appl. Catal. A: Gen. 378 (2010) 202–210.
[19] D.M. Mackay, D.L. Freyberg, P.V. Roberts, J.A. Cherry, A natural gradient experiment on solute transport in a sand aquifer. 1. Approach and overview of plume movement, Water Resour. Res. 22 (1986) 2017–2029.
[20] E.C. Butler, A.P. Davis, Photocatalytic oxidation in aqueous titanium dioxide in suspensions: the influence of dissolved transition metals, J. Photochem. Photobiol. A: Chem. 70 (1993) 273–283.
[21] C.-H. Liao, S.-F. Kang, F.-A. Wu, Hydroxyl radical scavenging role of chloride and bicarbonate ions in the H_2O_2/UV process, Chemosphere 44 (2001) 1193–1200.
[22] D. Klauson, S. Preis, E. Portjanskaja, A. Kachina, M. Krichevskaya, J. Kallas, The influence of ferrous/ferric ions on the efficiency of photocatalytic oxidation of pollutants in groundwater, Environ. Technol. 26 (2005) 653–662.
[23] L.L.P. Lim, R.J. Lynch, S.-I. In, Comparison of simple and economical photocatalyst immobilisation procedure, Appl. Catal. A: Gen. 365 (2009) 214–221.
[24] M. Rosell, S. Lacorte, D. Barcelo, Analysis, occurrence and fate of MTBE in the aquatic environment over the past decade, Trends Anal. Chem. 25 (2006) 1016–1029.
[25] P.A. Domenico, F.W. Schwartz, Physical and Chemical Hydrogeology, second ed., John Wiley and Sons Inc., U.S.A., 1997.
[26] M.L.B. Da Silva, P.J.J. Alvarez, Effects of ethanol versus MTBE on benzene, toluene, ethylbenzene, and xylene natural attenuation in aquifer columns, J. Environ. Eng. 128 (2002) 862–867.
[27] G.M.L. Riuz-Aguilar, J.M. Fernandez-Sanchez, S.R. Kane, D. Kim, P.J.J. Alvarez, Effect of ethanol and methyl-tert-butyl ether on monoaromatic hydrocarbon biodegradation: response variability for different aquifer materials under various electron-accepting conditions, Environ. Toxicol. Chem. 21 (2002) 2631–2639.
[28] C.W. Fetter, Contaminant Hydrogeology, second ed., Wiley and Sons. Inc., U.S.A., 1999.
[29] C.S. Chen, P.S.C. Rao, J.J. Delfino, Oxygenated fuel induced cosolvent effects on the dissolution of polynuclear aromatic hydrocarbons from contaminated soil, Chemosphere 60 (2005) 1572–1582.
[30] L.L.P. Lim, In-situ Photocatalytic Remediation of Organic Contaminants in Groundwater, Ph.D. Thesis, Univ. Cambs., U.K., 2010.